

The effects of realistic pancake solenoids on particle transport

X. Gu,

February 2011

Collider Accelerator Department
Brookhaven National Laboratory

U.S. Department of Energy

USDOE Office of Science (SC)

Notice: This technical note has been authored by employees of Brookhaven Science Associates, LLC under Contract No. DE-AC02-98CH10886 with the U.S. Department of Energy. The publisher by accepting the technical note for publication acknowledges that the United States Government retains a non-exclusive, paid-up, irrevocable, world-wide license to publish or reproduce the published form of this technical note, or allow others to do so, for United States Government purposes.

DISCLAIMER

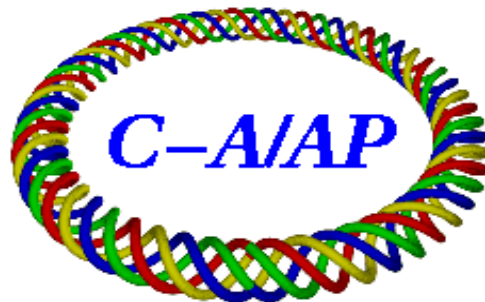
This report was prepared as an account of work sponsored by an agency of the United States Government. Neither the United States Government nor any agency thereof, nor any of their employees, nor any of their contractors, subcontractors, or their employees, makes any warranty, express or implied, or assumes any legal liability or responsibility for the accuracy, completeness, or any third party's use or the results of such use of any information, apparatus, product, or process disclosed, or represents that its use would not infringe privately owned rights. Reference herein to any specific commercial product, process, or service by trade name, trademark, manufacturer, or otherwise, does not necessarily constitute or imply its endorsement, recommendation, or favoring by the United States Government or any agency thereof or its contractors or subcontractors. The views and opinions of authors expressed herein do not necessarily state or reflect those of the United States Government or any agency thereof.

C-A/AP/#423

Feb. 2011

The Effects of Realistic Pancake Solenoids on Particle Transport

X. Gu, M. Okamura, A. Pikin, W. Fischer, Y. Luo



**Collider-Accelerator Department
Brookhaven National Laboratory
Upton, NY 11973**

Notice: This document has been authorized by employees of Brookhaven Science Associates, LLC under Contract No. DE-AC02-98CH10886 with the U.S. Department of Energy. The United States Government retains a non-exclusive, paid-up, irrevocable, world-wide license to publish or reproduce the published form of this document, or allow others to do so, for United States Government purposes.

1 **The Effects of Realistic Pancake Solenoids on Particle Transport**

2 X. Gu, M. Okamura, A. Pikin, W. Fischer, Y. Luo

3 Corresponding Author: X. Gu

4 Brookhaven National Laboratory, Upton, NY 11973

5 **Abstract**

6 Solenoids are widely used to transport or focus particle beams. Usually, they are assumed as being ideal
7 solenoids with a high axial-symmetry magnetic field. Using the Vector Field Opera program, we modeled
8 asymmetrical solenoids with realistic geometry defects, caused by finite conductor and current jumpers.
9 Their multipole magnetic components were analyzed with the Fourier fit method; we present some
10 possible optimized methods for them. We also discuss the effects of “realistic” solenoids on low energy
11 particle transport. The finding in this paper may be applicable to some lower energy particle transport
12 system design.

13 **Keywords:** realistic solenoids, multipole magnetic fields, particle transport

14

15 **1. Introduction**

16 Solenoids are used extensively for focusing and transporting the beams in modern accelerators [1-4].
17 Many high-energy particle detectors are equipped with superconducting (cold) solenoids [5-6], that
18 operate at very low temperatures. Meanwhile, many normal conducting (warm) solenoids [7-10] work
19 at room temperature.

20 To evaluate the effects of a solenoid on the beam’s parameters, we must calculate the magnetic field
21 [11] or transfer matrix [12-14]. Many researchers discussed ways of assessing magnetic fields, wherein
22 the fields are calculated on-axis [15] or off-axis [16], with an infinite solenoid [17-19], semi-infinite one
23 [20], or a finite one [21-22]. Some papers and textbooks concentrate on calculating the transfer matrix
24 [12-14]. When evaluating either of them, static magnetic fields produced by cold or warm solenoids
25 usually are assumed to be axially symmetric.

26 Nevertheless, many applications [23-24] require at the least an estimate of the solenoid’s multipole
27 magnetic fields with asymmetry, caused by the realistic solenoid structure. However, very few papers
28 cover this situation.

29 Moreover, although some effort [23-25] was devoted to ascertaining the magnetic fields of a solenoid’s
30 multipole components, it is important thoroughly to study the origins of these components, and to
31 devise methods of reducing them using the structure of the coil winding.

32 The pancake-type solenoid is a frequent choice for applications requiring inexpensive high-power
33 density. Their popularity mainly rests on the ability to connect its electricity in series and the water flow
34 in parallel.

35 In this paper, we address the mechanism that produces multipole magnetic fields in a pancake solenoid
36 and methods to optimize them. Our results demonstrate that the “realistic” solenoid dipole component

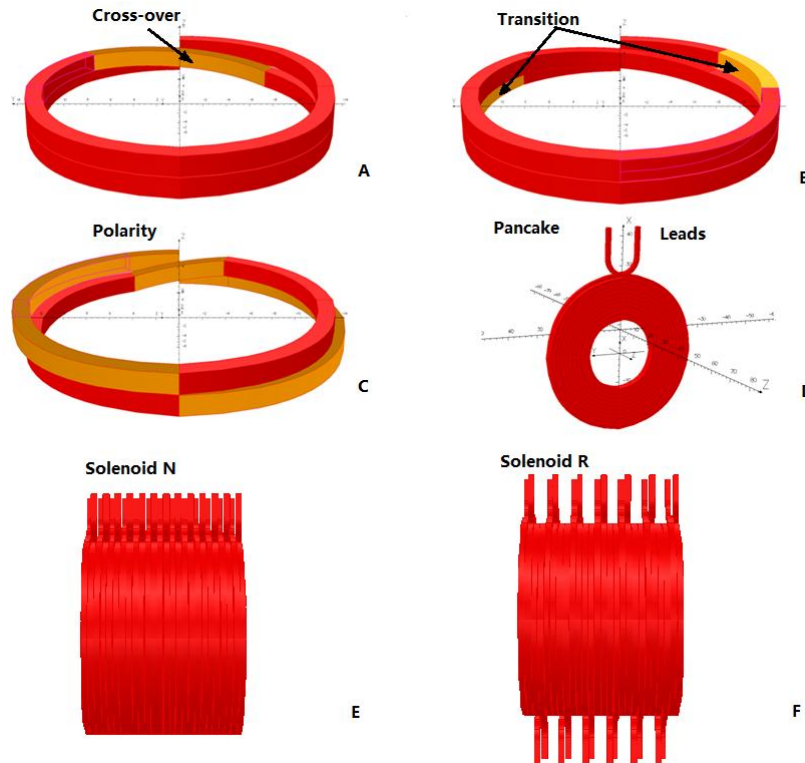
37 is reduced by 180 degrees by rotating the interval pancakes in this solenoid. This finding may be
38 applicable to transporting several species of lower energy, such as electrons [26-28], protons [29] and
39 ions [30-34], or for emittance compensation [23-24, 35] in photocathode electron guns.

40 We begin with a brief overview of warm solenoid structures, and then analyze the solenoid magnetic
41 fields with different structures. After that, we discuss the effects of one and two “realistic” solenoids on
42 the propagation of particle beams. Finally, some conclusions and recommendations for further study are
43 presented.

44 2. Structure of the Pancake Solenoid

45 The multipole magnetic field components of realistic solenoids are caused by their asymmetrical
46 construction, which includes cross over angles, transition angles, pancake polarity, leads, and pancake
47 rotation.

48 Pancake is the basic element of this kind of solenoid. One warm solenoid is constructed by assembling
49 several pancakes in different combinations. Fig. 1 shows the geometric structure of one pancake.



50

51

Fig. 1 Structure of a Pancake and Solenoid

52 One pancake consists of two spirals joined on their inner radius by a cross over (Fig. 1 A). Here, we
53 define the cross over angle as the half angle of the cross over conductor. Fig. 1 A and Fig. 1C have,
54 respectively, a 45° and a 22.5° cross over angle.

55 Each layer of the pancake’s spiral is almost a circle. A transition conductor connects one layer to another
56 one (Fig.1 B). The first inner layer must transit to the second layer before reaching the cross over

57 conductor. The transition is defined from the transition angle to the cross over angle. The transitions in
 58 Fig. 1 B and Fig. 1C, respectively, start from 90° to 45°, and 180° to 22.5°.

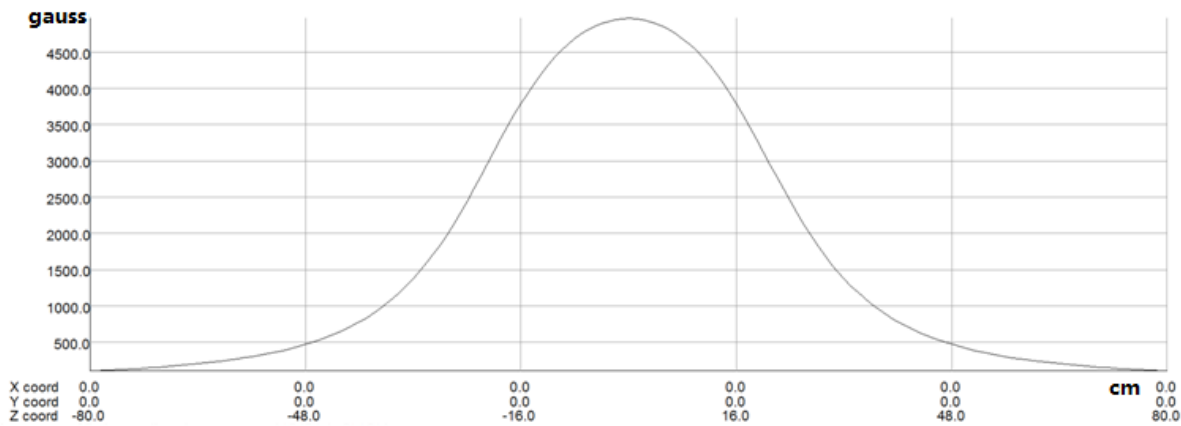
59 Each pancake can have its own polarity. Compared with Fig.1 B, Fig.1 C not only has a different cross
 60 over and transition angle, but also has an opposite polarity. After winding several layers, the resulting
 61 pancake with leads is illustrated in Fig.1 D.

62 One solenoid can have many pancakes that may have different polarities or different rotations. The
 63 solenoid named Solenoid N has same pancake polarity and rotation direction (Fig. 1 E); the solenoid
 64 called Solenoid R, has same pancake polarity but alternate pancake rotation (Fig. 1 F). In this paper, six
 65 of 13 pancakes are rotated by 180° alternately in Solenoid R. Solenoids that have same pancake rotation
 66 but alternate pancake polarity are named Solenoid P.

67 Accordingly, the solenoid with different cross over, transition angle, pancake polarity and pancake
 68 rotation can have different multipole magnetic field distributions. Furthermore, the leads of individual
 69 pancakes may affect these distributions.

70 3. Analysis Method

71 Using the different geometric parameters discussed in Section 2, we constructed several realistic
 72 solenoids modeling them via Vector Field Opera program. All have thirteen pancakes, each pancake with
 73 10 layers. Their inner- and outer- diameters are 234mm and 526mm, respectively. Their length is
 74 379.6mm. Fig. 2 illustrates the distribution of the longitudinal magnetic field strength of one of them.



75

76 Fig. 2 Solenoid and Its Longitudinal Field Bz

77 The multipole magnetic field components generated by such “realistic” solenoids are analyzed and
 78 compared by Fourier fit method.

79 In cylindrical coordinates, we can express the radial and azimuthal components of magnetic field B in
 80 the form [36-37]:

81
$$B_r(r, \theta) = \sum_{n=1}^{\infty} (b_n \sin(n\theta) + a_n \cos(n\theta)) \quad (1)$$

82
$$B_{\theta}(r, \theta) = \sum_{n=1}^{\infty} (b_n \sin(n\theta) - a_n \cos(n\theta)) \quad (2)$$

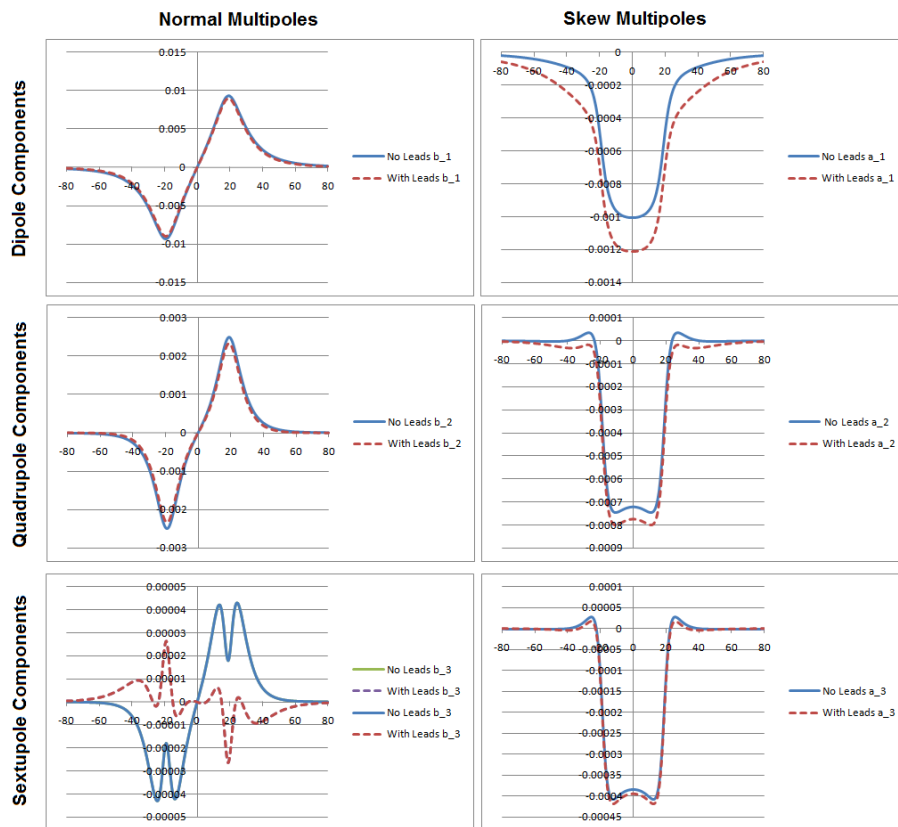
83 Where b_n is the amplitudes of the $2n$ pole normal term and a_n is the amplitudes of $2n$ pole skew term
 84 in the "European Convention".

85 The multipole magnetic field, B_θ can be computed on a reference radius R_{ref} at different longitudinal
 86 positions and fitted as Fourier series. Then, according to formula (2), the coefficients of this Fourier
 87 series are the multipole magnetic field components. The reference radius $R_{ref} = 75$ mm, and the
 88 longitudinal position from -80 cm to +80 cm are used in this paper. The original point of cylindrical
 89 coordinate was set at the center of the solenoid's geometry.

90 4. Multipole Components for Different Solenoid Structures

91 In this section, we calculate the normalized multipole magnetic field components for different solenoid
 92 structures. They are the solenoids with different leads, transition angles, cross over angles, pancake
 93 rotations and pancake polarities.

94 Figure 3 shows the multipole components for solenoids with and without leads.



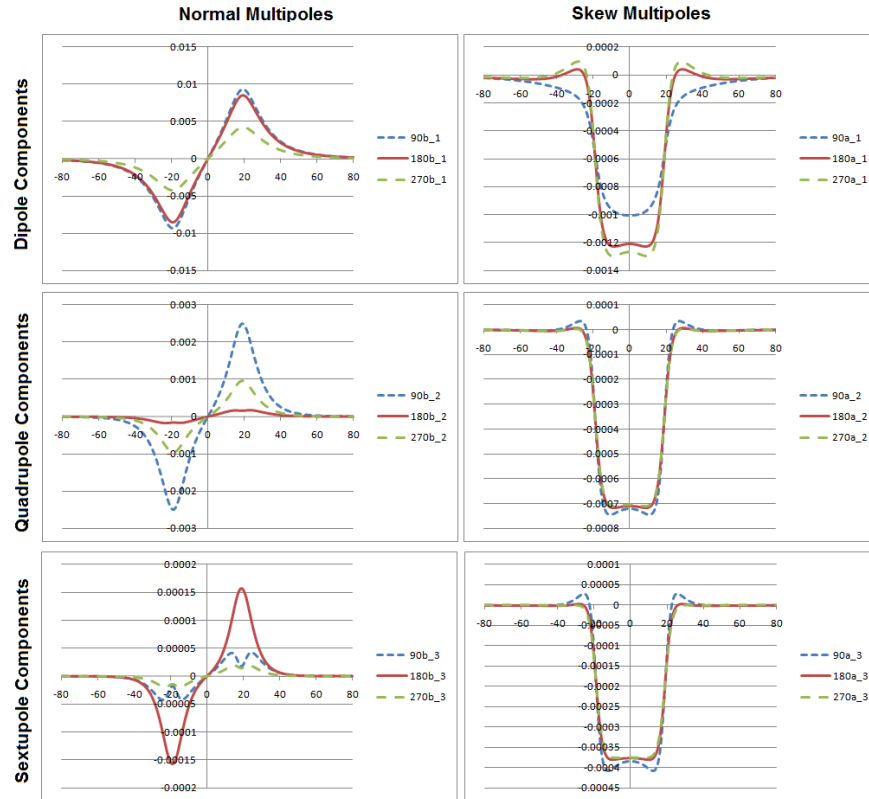
95

96 Fig. 3 Solenoids Multipole Components with and without Leads

97 In Fig. 3, the three rows respectively represent the dipole, qadrupole, and sextupole components; the
 98 two columns represent the normal (left) and skew (right) multipole components. The horizontal axis is
 99 the longitudinal position in units of centimeters and the vertical axis is the normalized amplitudes of the
 100 multipole component. Because the multipole components with $n > 3$ have lower magnetic field
 101 strength, only those with $n \leq 3$ are shown.

102 As evident from Fig. 3, the distribution of multipole component ($n \leq 3$) with and without leads have
 103 only a slight difference except for the normal sextupole magnetic field. For this reason, in further
 104 analyses we removed the leads from the models.

105 Figure 4 plots the calculated solenoid multipole components with different transition angles.



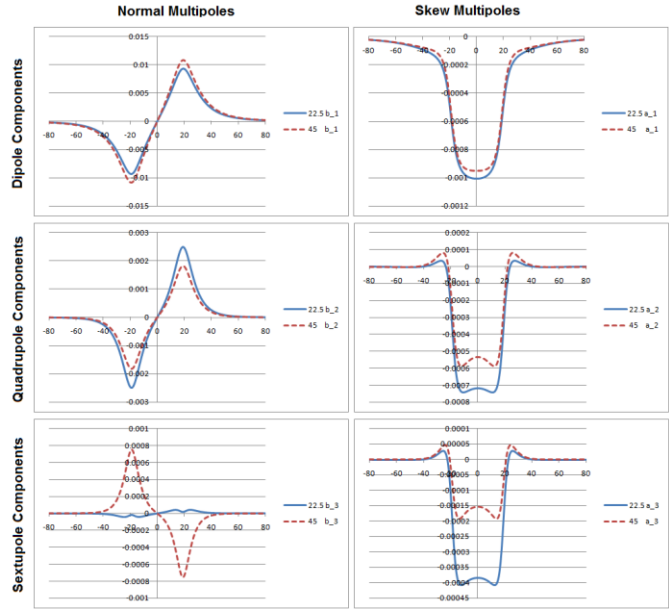
106

107

Fig. 4 Solenoids Multipole Components versus Transition Angles

108 With the same cross over angle (22.5°), we studied three solenoid structures with 90° , 180° and 270°
 109 transition angles. Fig. 4 reveals that different transition angles induce different distributions of high
 110 order component. Seemingly, the solenoid with the 270° angle has the minimum normal dipole
 111 component, while the solenoid with the 180° angle has the minimum normal quadrupole component.

112 The multipole components of solenoids with different cross over angles were computed and are plotted
 113 in Fig. 5.



114

115

Fig. 5 Solenoids Multipole Components versus Cross over Angle

116

In this instance, we changed the cross over angle from 22.5° to 45° and transition angle is 90°. Because conductor transits from the transition angle to the cross over angle, the length of transition conductor also changes. The effects of the cross over angle on multipole components are unclear.

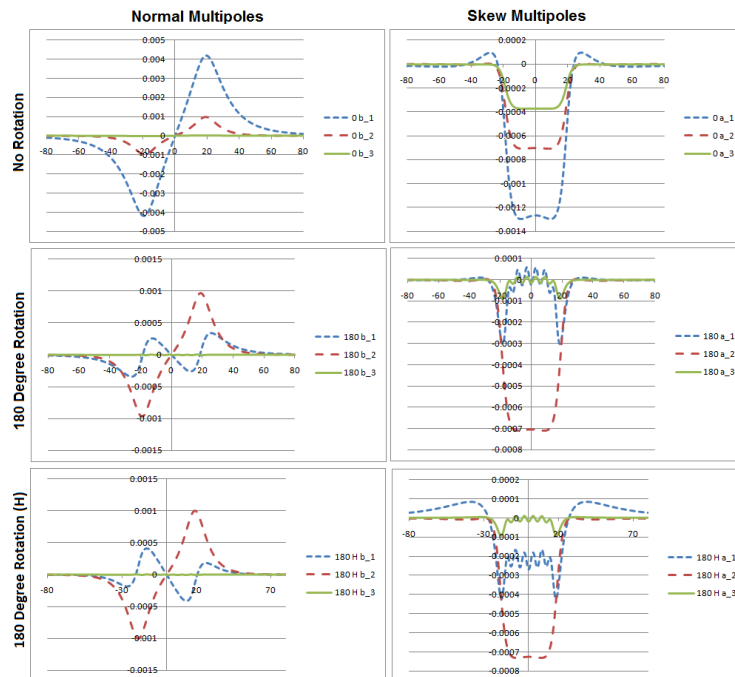
117

118

119

Figure 6 plots the calculated multipole components of solenoids with (Solenoid R) and without (Solenoid N) pancake rotation. The transition is set to 270° and the cross over angle is 22.5°.

120



121

122

Fig. 6 180° Rotation versus no Rotation

123

124 In Fig. 6, b (a) _1, b (a) _2 and b (a) _3 correspond, respectively, to normal (skew) dipole, quadrupole
125 and sextupole components. The first row is calculated with Solenoid N and the second with Solenoid R.

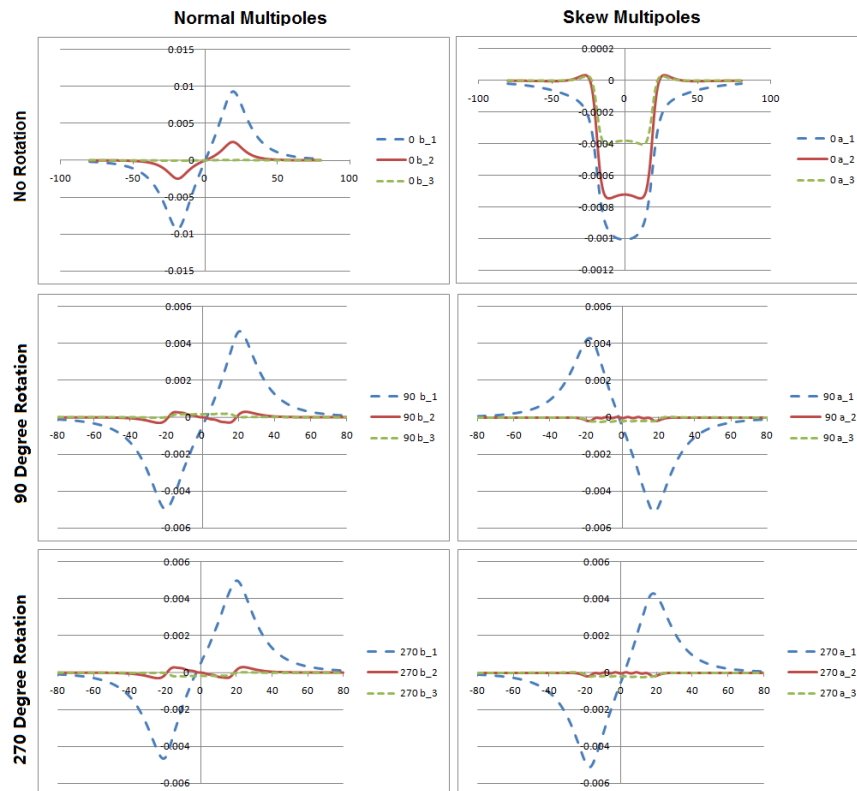
126 From second row in Fig. 6, we conclude that the 180° alternate rotation of pancakes in a normal
127 solenoid reduces the normal dipole component dramatically. This result is confirmed by the solenoid
128 with the 180° transition angle and 22.5° cross over angle. However, apparently it does not change the
129 normal quadrupole and sextupole components.

130 Nevertheless, for Solenoid R, it is difficult to assemble a coil with output wires pointing in opposite
131 directions. Besides, there should be some jumpers connecting these coils in series, and they also will
132 introduce some multipole components.

133 To resolve this problem, we changed the layers of seven non-rotated pancakes in Solenoid R from 10 to
134 9.5, so that all pancakes have the same azimuthal position. The simulation for this configuration is
135 shown as the third row in Fig. 6.

136 The normal dipole component can be reduced by using Solenoid R with a 180° rotation. The quadrupole
137 component can be optimized by 90° pancake rotation or 270° rotation; in this instance, the transition
138 angle is set to 90° and the cross over angle is 22.5°.

139 From Fig. 7, we note a reduction in both the normal quadrupole component and normal dipole
140 component. The skew quadrupole component also decreases, but the skew dipole component increases.

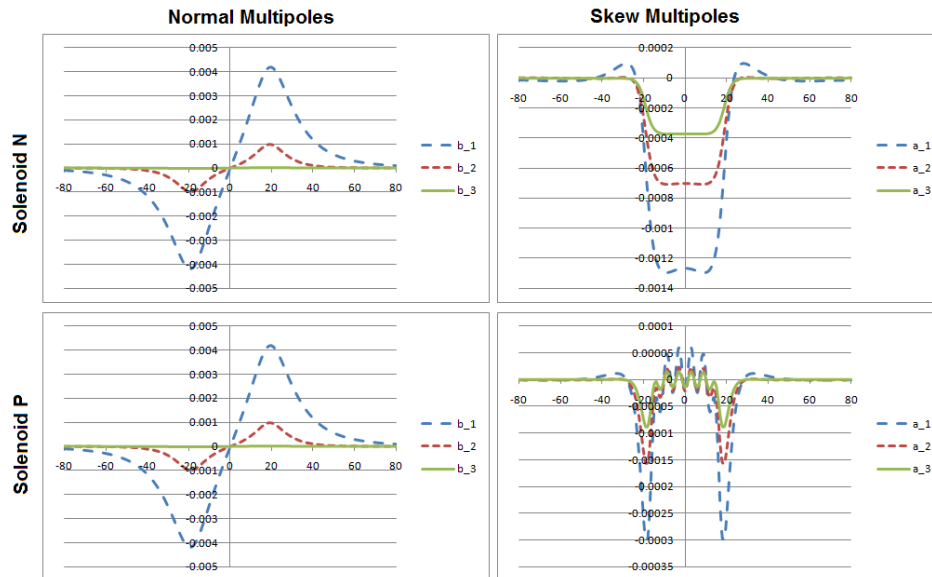


141

142

Fig. 7 Optimization of the Quadrupole Component

143 Finally, the components of the solenoid multipole magnetic field with (Solenoid P) and without (Solenoid N)
 144 N) polarity pancakes, were assessed and are presented in Fig. 8.



145
 146 Fig. 8 No Polarity versus with Polarity

147 This figure shows that in Solenoid P only the skew multipole components change; the normal multipole
 148 components do not.

149 According to different design requirements, we can optimize the normal dipole, quadrupole, and
 150 sextupole components and skew the dipole components by using different transition angles; thereafter
 151 further optimization is achieved different pancake rotation.

152 5. Beam Transport with a Realistic Solenoid

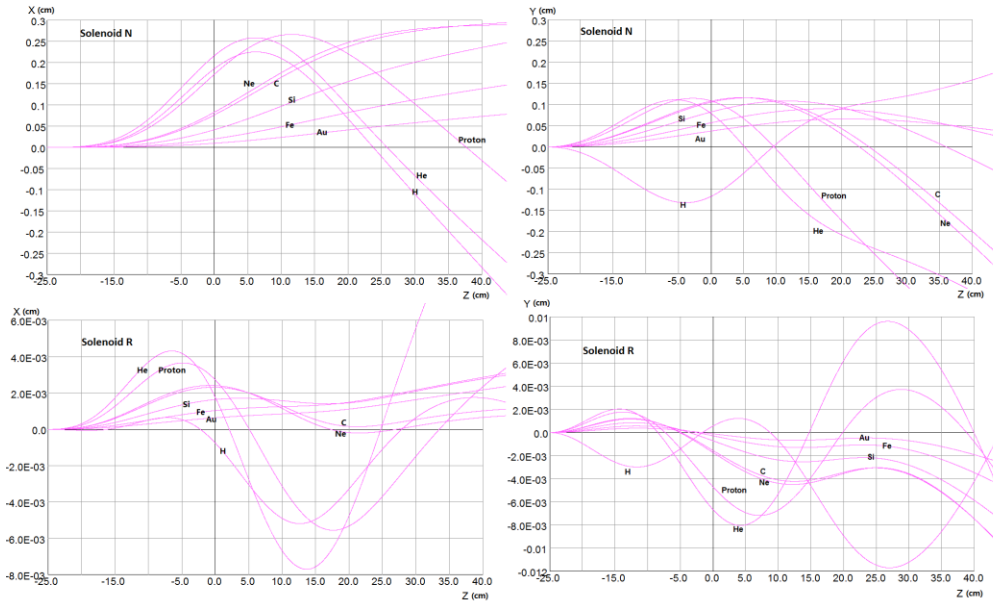
153 In this section, firstly, we discuss the detrimental effects of a single realistic solenoid on particle
 154 transport. Then we analyze the effects of two realistic solenoids on propagation of a particle beam.

155 The dipole component's field of a single realistic solenoid can deflect some kinds of particle trajectories
 156 at low energy. To verify this effect and find methods to improve it, we simulated the passage of some
 157 particles through a single Solenoid N and Solenoid R. These solenoids have the same dimensions, with a
 158 180° transition angle and a 22.5° cross over angle.

159 Table 1 Position Change for Different Particles

Particle	Atomic Number	Charge	Energy (kV)
Proton	-	+1	80
H	1	-1	50
He	2	+1	13
C	6	+5	102
Ne	10	+2	22
Si	14	+13	238
Fe	26	+20	442

160 The center of solenoid is set at Z=0, and their axis is oriented along the Z-axis. All particles start from Z=-
 161 25 cm on the solenoid axis. Table 1 lists the particle's parameters; their trajectories are illustrated in Fig.
 162 9.



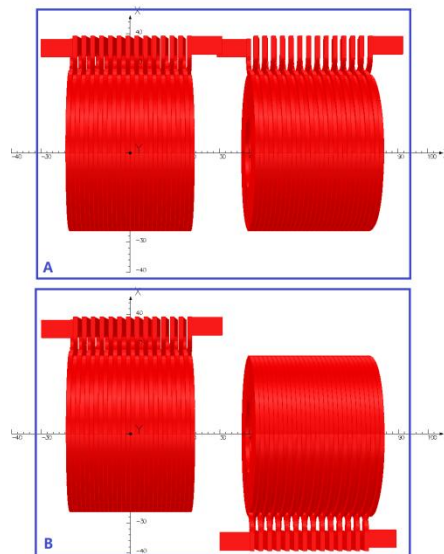
163

164

Fig. 9 Particle Trajectories with Normal and Rotated Solenoid

165 As Fig. 9 reveals, unlike the ideal solenoid, the particle's trajectories do not follow along the center axis
 166 when they pass through these realistic solenoids. From -25 cm to 40 cm, the particle trajectories of
 167 Solenoid R have at least 10 times smaller deviations in transverse amplitude than do those of Solenoid N.

168 Sometimes, the beam transport system has several contiguous solenoids. We discuss the effects of
 169 relative solenoid orientation on beam propagation for Cases A and Case B in Fig. 10 that have only two
 170 adjacent realistic solenoids.

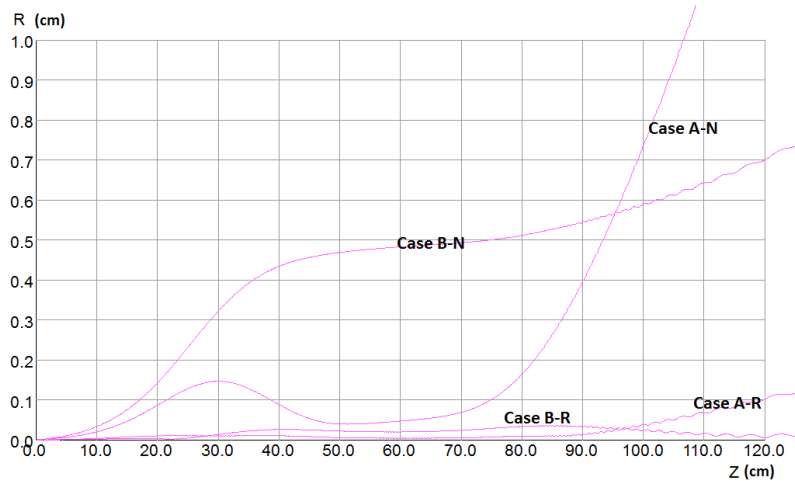


171

172

Fig. 10 Arrangement of the Two Solenoids

173 For Cases A and B, we use two kinds of solenoids, Solenoid N and Solenoid R; their configurations are
174 termed Case A-N, Case A-R, Case B-N, and Case B-R, respectively. The center of left solenoid is set to Z=0,
175 another solenoid's center is set to Z= 60 cm. In the simulations, a single electron starts from Z=0, and its
176 velocity is parallel to the solenoid's axis. The simulated trajectories for these four cases are shown in Fig.
177 11.



178

Fig. 11 Trajectories for Different Solenoid Arrangements

179

180 As depicted, Case B undergoes less angle change after passing through two solenoids than Case A; while
181 for both cases with Solenoid R, there is less change in angle and position than Solenoid N. Thus, when
182 designing a low energy beam transport system with solenoids, different beam requirements maybe
183 necessitate different solenoid configurations.

184 6. Discussion

185

186 In this paper, we presented some simulations with realistic solenoids and their affects on the transport
187 of low energy particle beam. Unlike the ideal solenoids, the realistic solenoids have high order
188 components that can deflect particle's trajectories. With the 180° alternate rotation of pancakes in the
189 normal solenoids, the normal dipole component can be reduced dramatically. Using these solenoids
190 (Solenoid R), we can design a low energy particle's transport system with less angle and position
191 deviation. Combined with the transfer maps [39], which include high order multipole field, these
192 simulations also can help us in understanding the particle's trajectories when they pass the realistic
193 solenoids.

194 However, there are more researches are needed on this topic. Firstly, the effects of cross over angles are
195 not very clear. Secondly, because there is a force placed on wire when winding the pancakes, the final
196 realistic transition angle and cross over angle may differ from their design value. This force may distort
197 them, and introduce more complex conductor geometry in pancakes. More research also is needed on
198 quadrupole and sextupole effects.

199 **7. Acknowledgment**

200

201 The authors acknowledge helpful discussions with Walter Shaffer and Jonathan Hock.

202

203 **References**

204

205 [1] A. Yamamoto, Y. Makida, R. Ruber, et al., Nucl. Instr. and Meth. A 584 (2008) 53 – 74.

206 [2] S.H. Aronson, J. Bowers, J. Chiba, et al., Nucl. Instr. and Meth. A 499 (2003) 480 – 488.

207 [3] S. Seletskiy, in: Proceedings of PAC07, Albuquerque, New Mexico, 2007, pp: 3109 – 3111.

208 [4] A.A. Efremov, E.K. Koshurnikov, Y.Y. Lobanov, et al., Nucl. Instr. and Meth. A 585 (2008) 182 – 200.

209 [5] L. Mirabito, Nucl. Instr. and Meth. A (2010), doi:10.1016/j.nima.2010.02.243

210 [6] D. Toprek, Y. Nosochkov, Nucl. Instr. and Meth. A 612 (2010) 260 – 273.

211 [7] S.J. Russell, Z.-F. Wang, W.B. Haynes, Phys. Rev. ST Accel. Beams. 8 (2005) 080401.

212 [8] R.J. Hayden, M.J. Jakobson, Nucl. Instr. and Meth. A 278 (1989) 394 – 396.

213 [9] S. M'Garrech, Nucl. Instr. and Meth. A 550 (2005) 535 – 542.

214 [10] E. Beebe, J. Alessi, S. Bellavia, et al., Rev. Sci. Instrum. 71 (2000) 893 – 895.

215 [11] D. B. Montgomery, Solenoid Magnet Design, John Wiley & Sons, Inc. New York, 1969.

216 [12] G. Xu, Phys. Rev. ST Accel. Beams. 7 (2004) 044001.

217 [13] D. Rubin, in: Alexander Wu Chao and Maury Tigner (Eds.), Handbook of Accelerator Physics and
218 Engineering, 2nd ed., World Scientific Publishing Co. Pte. Ltd. Singapore, 2002, pp.272 – 277.

219 [14] G. Franchetti, Phys. Rev. ST Accel. Beams. 4 (2001) 074001.

220 [15] C. Chia and Y. Wang, Phys. Teach. 40 (2002) 288 – 289.

221 [16] R. H. Jackson, IEEE Trans. Electron Devices 46 (1999) 1050 – 1062.

222 [27] V. Labinac, N. Erceg, D. Kotnik-Karuza, Am. J. Phys. 74 (2006) 621-627.

223 [18] O. Espinosa and V. Slusarenko, Am. J. Phys. 71 (2003) 953 – 954.

224 [19] K. Fillmore, Am. J. Phys. 53 (1985) 782–783.

225 [20] G. V. Brown and L. Flax, J. Appl. Phys. 35 (1964) 1764–1767.

226 [21] J. Farley and R.H. Price, Am. J. Phys. 69(2001) 751 – 754.

- 227 [22] V. I. Danilov, M. Ianovic, Nucl. Instr. and Meth. 94 (1971) 541 – 550.
- 228 [23] M. Ferrario, M. Migliorati, P. Musumeci, et al., in: Proceedings of EPAC 2006, Edinburgh, Scotland,
229 2006, pp. 169 - 171.
- 230 [24] J. Schmerge, LCLS Gun Solenoid Design Considerations (LCLS-TN-05-14), LCLS project, SLAC, 2005.
- 231 [25] A. Wolski, M. Venturini, in: Proceedings of EPAC2004, Lucerne, Switzerland, 2004, pp: 2185 – 2187.
- 232 [26] V. Shiltsev, K. Bishofberger, V. Kamerzhiev, et al., Phys. Rev. ST Accel. Beams. 11 (2008) 103501.
- 233 [27] D. Xiang, Y.C. Du, L.X. Yan, et al., Phys. Rev. ST Accel. Beams. 12 (2009) 022801.
- 234 [28] W. Fischer, Y. Luo, A. Pikin, etc, in: Proceedings of IPAC10, Kyoto, Japan, pp: 513 – 515.
- 235 [29] G. Ciavola, L. Celona, S. Gammino, et al., in: Proceedings of LINAC2002, Gyeongju, Korea, 2002, pp:
236 674 – 676.
- 237 [30] E. Lee, Nucl. Instr. and Meth. A 544 (2005) 187 – 193.
- 238 [31] R. Hollinger, P. Spädtke, Rev. Sci. Instrum. 79 (2008) 02B704.
- 239 [32] J. Alessi, D. Barton, E. Beebe, et al., in: Proceedings of LINAC2006, Knoxville, Tennessee, USA, 2006,
240 pp: 385 – 387.
- 241 [33] M. Eshraqi, G. Franchetti, A.M. Lombardi, et al., Phys. Rev. ST Accel. Beams. 12 (2009) 024201.
- 242 [34] J.H. Li , J.Y. Tang, Nucl. Instr. and Meth. A 574 (2007) 221 – 225.
- 243 [35] J.B Rosenzweig, A.M Cook, M.P. Dunning, et al., in: Proceedings of 2005 Particle Accelerator
244 Conference, Knoxville, Tennessee, 2005, pp. 2624 – 2626.
- 245 [36] A. K. Jain, in: Turner, S [ed], CAS - CERN Accelerator School : Measurement and Alignment of
246 Accelerator and Detector Magnets, Geneva, CERN, 1998, pp. 1 – 26.
- 247 [37] A. K Jain, P. Wanderer, in: Alexander Wu Chao and Maury Tigner (Eds.), Handbook of Accelerator
248 Physics and Engineering, 2nd ed., World Scientific Publishing Co. Pte. Ltd. Singapore, 2002, pp.409 – 414.
- 249 [38] J. Back, J.Pozimski,P. Savage, et al, in: Proceedings of IPAC10, Kyoto, Japan, pp: 648 – 650.
- 250 [39] C. E. Mitchell and A. J. Dragt, Phys. Rev. ST Accel. Beams. 13 (2010) 064001.